



Subcritical water hydrolysis of sugarcane bagasse: An approach on solid residues characterization

D. Lachos-Perez^a, F. Martinez-Jimenez^a, C.A. Rezende^b, G. Tompsett^c, M. Timko^c, T. Forster-Carneiro^{a,*}

^a School of Food Engineering, University of Campinas (UNICAMP), Rua Monteiro Lobato, n.80, 13083-862 Campinas, SP, Brazil

^b Institute of Chemistry, University of Campinas, UNICAMP, 13083-862 Campinas, SP, Brazil

^c Department of Chemical Engineering, Worcester Polytechnic Institute, 100 Institute Road, Goddard Hall 123, Worcester, MA 01609, United States

ARTICLE INFO

Article history:

Received 21 August 2015

Received in revised form 8 October 2015

Accepted 28 October 2015

Available online 31 October 2015

Keywords:

Sugarcane bagasse

Reducing sugars

Subcritical water hydrolysis

FESEM

DRIFTS

ABSTRACT

Reducing sugars obtained from sugarcane bagasse, as a waste biomass energy precursor, can be further transformed into fuel alcohol by fermentation or gaseous fuel by gasification. In this work, subcritical water process was used as an environmentally friendly solvent for the hydrolysis of sugarcane bagasse with the aim of producing reducing sugars using residue bagasse from a sugarcane biorefinery. Hydrolysis in subcritical water performance was studied under semi-continuous unit conditions in a 110 mL reactor. Hydrolysis was carried out using different sample loadings (3 and 5 g), flow-rates (9 and 12.5 mL min⁻¹), temperatures (100, 150, 200 and 250 °C) and pressures (5, 10, and 15 MPa). The highest reducing sugar yields were obtained at temperature above 200 °C, with the highest reducing sugar yield reaching 15.5%. Scanning electron microscopy was used to analyze the sugarcane bagasse undergoing hydrolysis. Diffuse reflectance infrared spectroscopy was used to characterize the residual solids, with results consistent with the removal of hemicellulose during hydrolysis.

© 2015 Elsevier B.V. All rights reserved.

1. Introduction

Increasing energy demands and heavy consumption of non-renewable fossil fuels have emphasized the development and utilization of lignocellulosic biomass as a sustainable source for renewable energy production. In particular, conversion of biomass to high-performance biofuels (e.g. bioethanol, biohydrogen and biogas) has recently received increasing interest [1]. As an agricultural biomass waste, sugarcane bagasse is abundant, inexpensive and readily available in sugarcane mills. Due to the lack of cost-effective treatment and recycling approaches, most straws are burned or discarded in the field. As a consequence, environmental pollution, especially high levels of particulate material (i.e. PM2.5), has become a serious issue associated with bagasse disposal [2].

Sugar and ethanol production is an important sector of the Brazilian economy, and Brazil is the leading worldwide sugarcane producer. For example, the 2013–2014 sugarcane harvest produced 653 million tons, from which 27 billion liters of ethanol and 37 million tons of sugar were obtained [3]. Sugarcane processing

generates a large amount of residue. Sugar mills generate approximately 270–280 kg of 50% moisture content bagasse per metric ton of processed sugarcane, representing an annual production of approximately 200 million tons of bagasse. Sugarcane bagasse composition is reported as: 19–24% lignin, 27–32% hemicellulose, 32–44% cellulose, and 4.5–9% ash [4]. The potential to convert bagasse cellulosic and hemicellulosic fractions to fermentable sugars has been investigated by several research groups [5–7]. However, process optimization is still needed before second generation bioethanol can be produced at an industrial level. The difficulty is production of simple, fermentable sugars from the bagasse, since breaking down the lignocellulosic complex is usually achieved by energy intensive conversion (hydrolysis) of the cellulose and hemicellulose components of the biomass into sugars.

Classical technologies employed for the hydrolysis of feedstock into fermentable sugars usually rely on acid, alkaline or enzymatic catalysts [8–10]. Unfortunately, all these technologies have drawbacks. Acid and alkali hydrolysis are corrosive, use toxic solvents, and require neutralization of the medium after the reaction, generating solid wastes [11]. The main drawbacks associated with enzymatic hydrolysis are the long reaction time needed to achieve full hydrolysis, the cost of the enzymes, and the quantities of enzymes required.

* Corresponding author.

E-mail address: forster@fea.unicamp.br (T. Forster-Carneiro).

Subcritical water, also known as hydrothermal water, liquid hot water, and hot-compressed water, is defined as hot water at temperature ranging between 100 and 374 °C and maintained under sufficiently high pressures to maintain water in its liquid state. Subcritical water has attracted considerable attention due to its unique and temperature-tunable properties of density, viscosity, dielectric constant, ionic product, diffusivity, electric conductance, and solvent ability [12]. Moreover, subcritical water is an environmentally innocuous, non-toxic, and safe solvent.

Subcritical water hydrolysis (SWH), also termed hydrothermal liquefaction, hydrothermolysis, and aquathermolysis, has potential for breaking down the cellulose and hemicellulose biopolymers into simple sugars and small molecules for downstream fermentation or gasification. High density of liquid water held at high temperatures promotes the hydrolysis reactions required for conversion of biomass biopolymers into simple sugars. Using water as the reactant reduces some of the drawbacks of conventional methods. Compared to acid, alkali, or enzyme hydrolysis, the main advantages of SWH are that it requires minimal biomass pre-treatment (milling, drying, etc.), generates less waste and fewer degradation products, requires shorter reaction times, has fewer corrosion problems, and requires no toxic or expensive solvents.

Given its importance in Brazil and elsewhere, the focus of this work was valorization of sugarcane bagasse using SWH. We envision SWH as the first stage of a process to produce reducing sugars that then, on a second stage, could be gasified to generate an energy rich gas. This approach overcomes issues with the continuous feed of solids to the high-temperature and high-pressure gasification reactor. The SWH reaction can be performed semi-continuously in several parallel reactors to simulate a continuous flow to the gasifier. The objective of the study was to characterize the composition profile of the liquid hydrolysis products including measurement of liquid-phase pH and total reducing sugars (TRS). In particular, two reactor protocol were examined: (1) semi-continuous SWH and (2) semi-continuous SWH coupled with a static “holding” period. To understand more fully the dynamics of the decomposition process, we analyzed the solid residues using field emission scanning electron microscopy (FESEM) to investigate cell wall disruption that occurs during SWH and diffuse reflectance infrared Fourier transform spectroscopy (DRIFTS) to study composition changes.

2. Materials and methods

2.1. Raw material

Dry sugarcane bagasse was donated by the Brazilian Bioethanol Science and Technology Laboratory (CTBE, Campinas, SP, Brazil). The bagasse was stored at –18 °C prior to further experiments and then it was comminuted in a knife mill (Marconi, model MA 340, Piracicaba, Brazil) equipped with a 1 mm sieve before it was used as sample in the experiments. Distilled water was used in all experiments.

2.2. Sugarcane bagasse characterization

The sugarcane bagasse was characterized in triplicate according to the methodologies recommended by National Renewable Energy Laboratory, biomass laboratory analytical procedure (described in technical report – NREL/TP-510-42618-42619-42621-42622-42625). Table 1 presents result of CHNS analysis and characterization data of sugarcane bagasse.

Table 1
Proximate analysis and elemental analysis of sugarcane bagasse.

Composition	%wb
Proximate analysis	
Moisture	9.136 ± 0.529
Ashes	2.023 ± 0.069
Extractives in water	4.110 ± 0.466
Extractives in ethanol	1.640 ± 0.165
Protein	1.530 ± 0.092
Acid soluble in lignin	3.513 ± 0.224
Acid insoluble in lignin	23.456 ± 0.620
Elemental analysis	
Carbon	43.1 ± 0.1
Hydrogen	5.7 ± 0.6
Nitrogen	0.51 ± 0.02
Oxygen (by difference)	50.69

Dados are expressed as mean ± standard deviation ($n=3$).

2.3. Experimental pilot-plant for hydrolysis and gasification in sub/supercritical water

A schematic diagram of the semi-continuous pilot-plant is shown in Fig. 1. The pilot-plant was built to hydrolyze and gasify lignocellulosic biomasses using either sub- or supercritical water. The apparatus consists of two reactors, termed “reactor 1” (with an internal volume of 110 mL) and “reactor 2” (790 mL). The maximum working conditions of reactor 1 are 300 °C and 42 MPa and for reactor 2 they are 600 °C and 42 MPa. Reactor 1 is constructed of 316 stainless-steel and capped with gasket filters (average pore size 300 μm) to retain sample particles. Reactor 1 is heated by an electric heating system type jacket (1500 W) and insulated by ceramic fiber. Reactor 2 (stainless-steel 316; 220 mm e.d. × 610 mm length) is a serpentine (4.5 m of length, spiral shape) tube. Inconel 625 was used as the material of construction; this material is commonly used in supercritical water gasification (SCWG) [13–15]. Inconel material contains nickel as the major component, which is known to be a good catalyst for methanation [16,17]. Reactor 2 is heated by an electric heating system with three resistors 1500 W each, located on the top, bottom and center of the vessel and insulated by ceramic fiber.

A liquid high pressure pump (Dual piston pump, model Prep 36 Pump, Apple Valley, MN, USA) was used to deliver water to the reactors. The pressure in the system was controlled by a back-pressure regulator (High-Pressure Piston-Sensing Back-Pressure Regulators, KHB Series, Lafayette, LA) and measured by two manometers. The reaction temperature was monitored by thermocouple (type K) outlet of the reactors 1 and 2. The hot effluent fluid exiting the reactor 1 was cooled to a temperature less than 30 °C in a stainless steel shell-and-tube heat exchanger coupled to a thermostatic bath (Marconi, model MA-184, Piracicaba, SP, Brazil) operating at –10 °C (using ethylene glycol 50% as the coolant.) The rapid cooling assures that the reaction is quenched after reaction. The liquid products were collected in a gas–liquid separator. The flow of gas products was measured with a mass flowmeter (Aalborg, model # GFM 17, 0–100 mL min^{–1}) and then collected in a stainless steel gas collector with a safety valve and volume of 300 mL.

2.4. Hydrolysis apparatus and protocol

To validate the new pilot-plant, trial runs were performed at 2.5 MPa and 100 °C; the reaction pressure was kept sufficiently high to prevent formation of a water vapor.

Hydrolysis tests were performed following two procedures. In the first step, either 3 or 5 g of raw material were used and the reactor pressure was set to either 5 or 10 MPa by introducing pressurized water into the system. Complete process conditions are

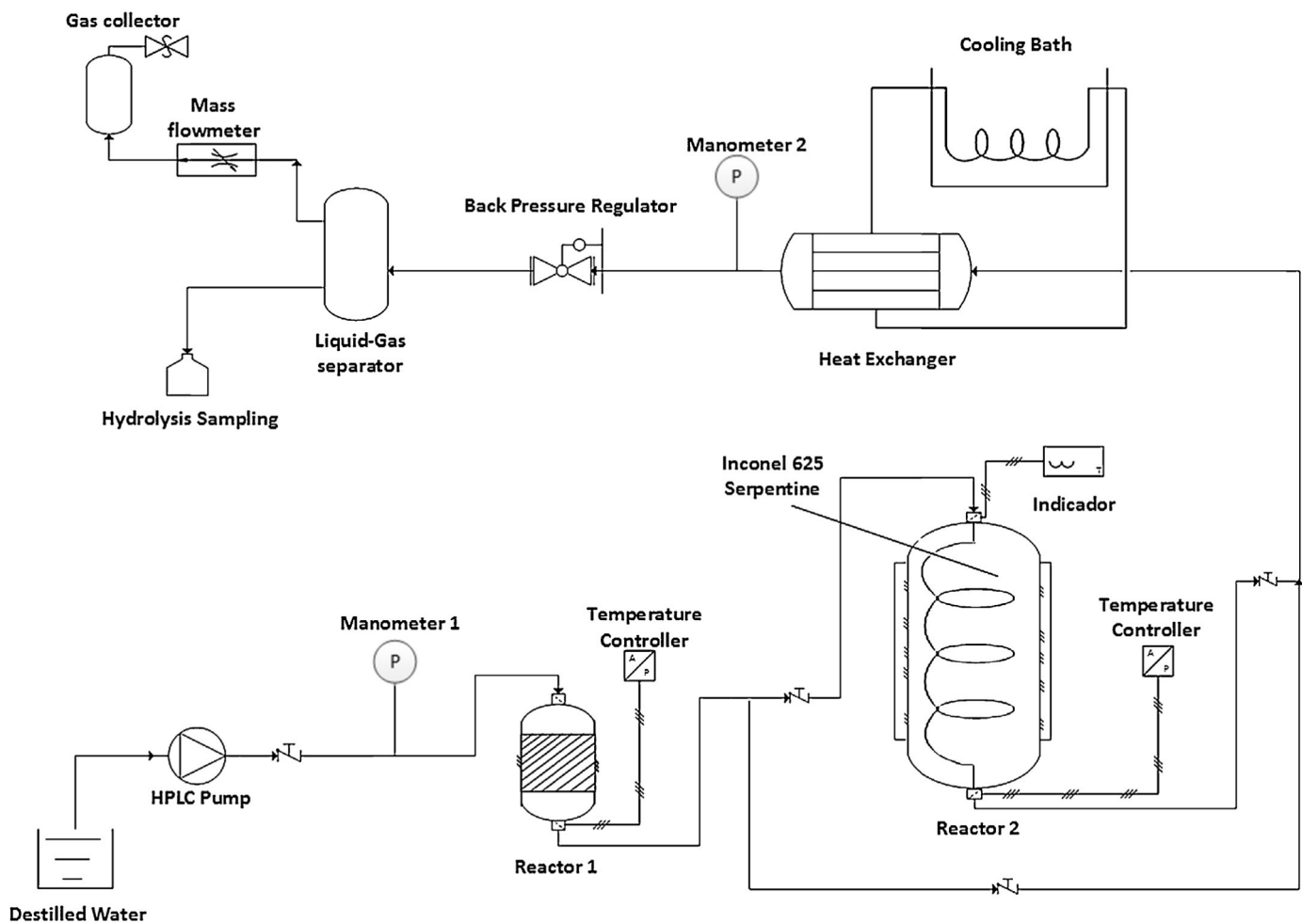


Fig. 1. Schematic diagram of experimental apparatus.

shown in **Table 2**. Prior to hydrolysis, distilled water was delivered to the system at room temperature to remove air and water-soluble substances. The dynamic period of the process was started by pressurizing the system and pumping water at the set-point flow rate (9 mL min^{-1}) through the system for 22 min. The temperature at the exit the reactor 1 was set at process temperature (100, 150, 200, and 250°C). Temperature stabilized after about 10–20 min, and time required to reach temperature stability is termed the “preheating time”. To assure that there was no hydrolysis of hemicellulose before reaction commenced; one sample was collected and analyzed during the preheating time. Once the stable operating temperature had been reached, liquid hydrolysate samples were collected every 2 min for the remainder of the experiment.

Table 2
Reactor conditions of sugarcane bagasse hydrolysis with subcritical water.

Units	Step 1			
	1	2	3	4
Mass (g)	5	5	3	3
Reactor outlet temperature ($^\circ\text{C}$)	100	150	200	250
Pressure (MPa)	10	10	5	5
Water flow rate (mL min^{-1})	9	9	9	9
Process time (min)	22	22	22	22
Water density (kg/m^3)	963	922.4	867.4	800.3
Water residence time in the reactor (min)	10.9	10.4	9.8	9

In the second step of experiments, the amount of raw material was maintained constant, at 5 g and the pressure was set at either 10 and 15 MPa. Prior to hydrolysis, distilled water was delivered to the system at room temperature to remove the air and water-soluble substances. Once the system was pressurized, the pump was stopped, which we called “static time”; the reaction temperature was increased to the set point ($150, 200^\circ\text{C}$) and the dynamic period was started by initiating flow (12.5 mL min^{-1} , measured at the pump head at laboratory conditions) through the reactor for 20 min. The reaction temperature was taken at a thermocouple positioned at the reactor outlet, and the pressure was taken at several locations in the system. At the start of the dynamic process, the temperature required approximately 15–18 min to stabilize. During the run, hydrolysate samples were collected every 2 min. **Table 3** summarizes the reactor conditions tested during this study.

All experiments were performed in duplicate, and yields are reported as average values, in wet basis, throughout the text. The fluid residence time (τ) was estimated by:

$$\tau = \frac{V_R \rho_R(T, P)}{v_0 \rho_0} \quad (1)$$

where V_R is the reactor fluid volume (m^3), v_0 is the volumetric liquid flow rate (25°C), ρ_0 is the density of the liquid feed (distilled water: 1080 kg/m^3), and ρ_R is the density of the fluid at the reactor 1 temperature and pressure estimated using NIST steam tables [18]. Eq. (1) assumes the fluid stream is at the reactor set-point temperature

Table 3

Reactor conditions of sugarcane bagasse hydrolysis with subcritical water.

Units	Step 2	
	1	2
Mass (g)	5	5
Reactor outlet temperature (°C)	150	200
Pressure (MPa)	10	15
Water flow rate (mL min ⁻¹)	12.5	12.5
Process time (min)	20	20
Water density (kg/m ³)	922.4	874.7
Water residence time in the reactor (min)	7.5	7.1

and pressure and does not account for density changes associated with temperature non-uniformity inside the reactor. The presence of SWH decomposition products in the reaction mixture was not factored into the residence time calculation, but since more fermentable sugars products are expected to be formed compared to the amount of water consumed, the residence time calculated by Eq. (1).

The severity factor (R_0), first proposed by Overend et al. [19] and Chornet and Overend [20], has been useful for modeling pseudo first order reaction rates as the combined influence of of temperature and residence time.

$$R_0 = t \exp\left(\frac{T - 100}{14.75}\right) \quad (2)$$

where t is the resident time (min), T is temperature (°C), 100 is the temperature of reference and 14.74 is an empirical parameter related with activation energy, assuming pseudo first order kinetics. The results are usually represented as a function of $\log(R_0)$.

2.5. Hydrolysate analysis

2.5.1. Determination of pH

The pH of the hydrolysates was determined using a digital pHmeter (Digimed, model DM-22, Santo Amaro, Brazil).

2.5.2. Total reducing sugar determination

The TRS content of the hydrolysate, was determined by the colorimetric method proposed by Somogyi–Nelson (SN) [21,22]. Two reactant solutions were prepared, SN-I and SN-II. The hydrolysate was subjected to acid hydrolysis to decompose sugar oligomers into monomers prior to detection as TRS. After the coloring reaction, sample absorbance at 540 nm was measured using a spectrophotometer (Hach, modelo DR/4000U, São Paulo, Brazil). The concentration of TRS was calculated using an external calibration curve based on standard glucose solutions (20, 60, 100, 140, 200, 300 and 400 mg/L), and expressed as glucose equivalents [5]. In some cases, hydrolysis product mixtures were diluted with distilled water prior to the absorbance measurement to remain within the instrumental calibration range.

2.6. Statistical analysis

The variance (ANOVA) of the results was evaluated using the software Statistica for Windows 6.0 (Statsoft, Inc., USA). The significant differences at level of 5% ($p \leq 0.05$) were analyzed through the Tukey's test.

2.7. The solid residue

After SWH, the residual solids contained in reactor 1 were transferred to a Petri dish, taking particular care to prevent loss. The amount of solid residue was determined by the difference between the initial amount of raw materials and the final residue remaining

in the reactor at the end of the process, using a digital analytical balance (Mettler Toledo, model: AB204, Switzerland).

2.7.1. Field emission scanning electron microscopy (FESEM)

The microstructure of the surface of sugarcane bagasse was analyzed before and after subcritical water hydrolysis (100 and 150 °C). The FESEM equipment was a scanning electron microscope, equipped with a field emission gun (Quanta 650, FEI, Hillsboro, OR, USA). Prior to analysis, the samples were coated with gold in a SCD 050 sputter coater (Oerlikon-Balzers, Balzers, Liechtenstein). Both equipment were available at the National Laboratory of Nanotechnology (LNNano), located in Campinas, SP, Brazil. Analyses of the sample surfaces were performed under vacuum, using a 5 kV acceleration voltage.

2.7.2. Diffuse reflectance infrared Fourier transform spectroscopy (DRIFTS)

Infrared spectra of sugarcane bagasse residues were collected using a Thermo Nicolet Magna 560 equipped with a SpectraTech DRIFTS cell. Spectra were obtained over the range from 4000 to 400 cm⁻¹, at a resolution of 2 cm⁻¹ and an accumulation of 96 scans. Multiple scans were obtained for each sample and averaged spectra are presented here. The DRIFTS cell was continuously purged with dry nitrogen 10 min prior to measurement to remove atmospheric CO₂ and H₂O that would interfere with the spectrum.

3. Results and discussion

3.1. Total reducing sugars yield

Literature [23–25] indicates that reaction temperature is the most important process parameter for SWH, with increasing temperature favoring biopolymer degradation at the cost of reduced recovery of TRS due to sugar decomposition. Accordingly, we focused our attention on studying the effects of SWH on TRS yield, with secondary experiments performed to investigate the influence of reaction pressure.

The TRS yields obtained at different conditions of temperature and pressure are shown in Table 4. A statistical analysis of variance ($p < 0.05$) was performed to evaluate the effect of temperature and pressure on TRS yield for step 1. The Tukey test showed that of the highest yield was obtained at 200 °C, and the yields of these operation conditions were statistically different ($p \leq 0.05$) compared to those obtained at 5 MPa/200 °C and 10 MPa/150 °C. The lowest yield was achieved at 10 MPa and 100 °C, consistent with the low hydrolysis rates expected at this low reaction temperature [26]. TRS yield (g glucose/100 g carbohydrate) increased from 100 °C (0.22%) to 150 °C (3.32%) to 200 °C until 250 °C (13.01%) for all pressures tested here [25]. This behavior can be explained by the effects of temperature on hydrolysis rates. Hemicellulose is hydrolyzed at 190–230 °C [27,28] while modest cellulose hydrolysis takes place below 230 °C [29,30].

Table 4

Total reducing sugar yield obtained by SWH in different conditions from sugarcane bagasse.

	Temperature (°C)	Pressure (MPa)	TRS (%)
Step 1	100	10	0.219 ± 0.040a
	150	10	3.318 ± 0.008b
	200	5	9.2 ± 1b
	250	5	13.0 ± 0.4c
Step 2	150	10	11.0 ± 0.4
	200	15	15.5 ± 1.0

Results are expressed as mean ± standard deviation of the analysis. Different letters in the same column indicate that the means differ significantly by Tukey test ($p \leq 0.05$).

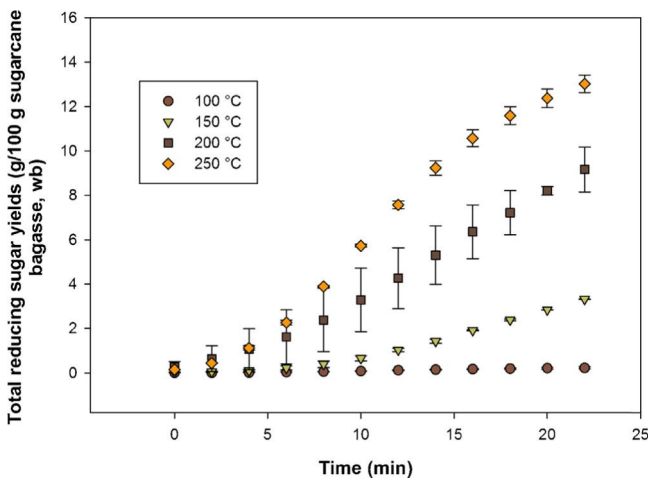


Fig. 2. Effects of reaction temperatures on total reducing sugar yields from sugarcane bagasse by subcritical water hydrolysis, step 1.

In general, reaction pressure used for SWH has not been shown to be a key parameter for determining TRS yield [31,32]. Consistent with the literature, pressure had an insignificant effect on the TRS yield, for the conditions examined here.

3.2. Effects of temperatures on total reducing sugar yields from sugarcane bagasse by subcritical water hydrolysis

Fig. 2 shows that the yield of TRS increases as the temperature increases. As expected [26,30,33,34], negligible sugar yields are obtained at 100 and 150 °C. This is consistent with the literature data which indicate that the hydrolysis of hemicellulose contained in most biomass types does not begin undergoing hydrolysis until the temperature exceeds 170 °C. The TRS yields reached were 9.15% and 13% at 200 and 250 °C, respectively. The increasing sugar yield obtained with increasing temperature can be attributed primarily to thermal effects on hydrolysis kinetics [35,36] and secondarily to the increased self-ionization constant of water. The increased self-ionization constant leads to increased concentrations of both H⁺ and OH in the reaction mixture, thereby facilitating the acid-catalyzed hydrolysis of cellulose and hemicellulose [37].

The highest TRS yields were obtained in step 2, as shown in Fig. 3. TRS yields reached 11% and 15.5% after 20 min held at 150 and 200 °C, respectively. In the second set of experiments, the

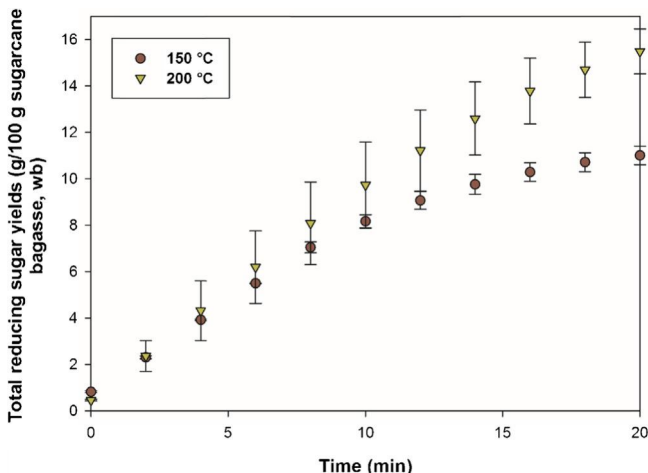


Fig. 3. Effects of reaction temperatures on total reducing sugar yields from sugarcane bagasse by subcritical water hydrolysis, step 2.

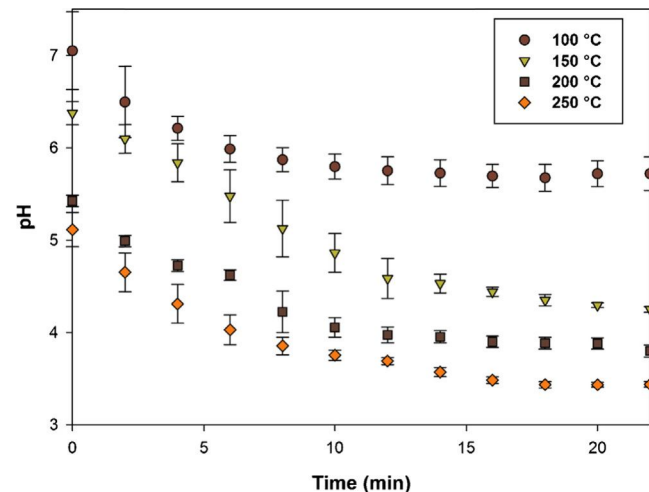


Fig. 4. The pH of the hydrolysates of sugarcane bagasse obtained by subcritical water hydrolysis at different temperatures, step 1.

reactor 1 jacket (reactor 1 outlet) temperature was adjusted to 150 and 200 °C; the dynamic period of the process was started by pumping water at the experimental flow rate through the system for 20 min. After the start of the dynamic period, the temperature at reactor 1 exit slowly increases until stabilization after 15–18 min; the results are expressed throughout the text as the reactor outlet temperature. Fig. 3 also shows a slight increase of the TRS yield with increasing water flow rate (12 mL) as compared with step 1 (9 mL). This is probably due to the lower residence time in reactor 1, which decreases the time for sugars degradation [5,38]. Similar behavior was observed during the subcritical water hydrolysis of corn stover and Citrus junos peel under semi-batch conditions [39,41].

3.3. pH of the aqueous solution

Fig. 4 shows that the pH of the hydrolysate recovered after subcritical water reaction decreased as hydrolysis temperature increased, for step 1; obviously, decreasing pH indicates the presence of acidic materials, probably organic acids in the aqueous hydrolysate solution. These organic acids provide acidic protons to catalyze subsequent hydrolysis of monomers and oligomers as an autocatalytic process [35]. Degradation products typically found in the hydrolysates include acetaldehyde, acetic acid, hydroxyacetone, acetone, acetylacetone, 2-acetylfuran, acrylic acid, 1,2,4-benzenetriol, dihydroxyacetone, erythrose, formic acid, furfural, glyceraldehydes, glycolaldehyde, glycolic acid, 5-hydroxymethyl furfural (5-HMF), lactic acid, levulinic acid, levoglucosan, 5-methyl furfural, pyruvaldehyde, solid precipitate ("humic solid") and gaseous products [42]. The degradation of monosaccharides into small molecules (e.g. 5-hydroxymethylfurfural (C₆H₆O₃) and furfural (C₅H₄O₂)) proceeds with the stoichiometry shown in the following equations:



Due to organic acid formation, the pH of the hydrolysate decreases strongly with increasing temperature and slightly with increasing hydrolysis time, as shown in Fig. 4. The trend can be explained because the operational conditions required to break down the lignocellulosic complex are severe enough to promote the degradation of fermentable sugars simultaneously with the hydrolytic process [5]. Also, degradation of hemicellulose release acetic acid due to hydrolysis of acetyl side chains. A greater drop

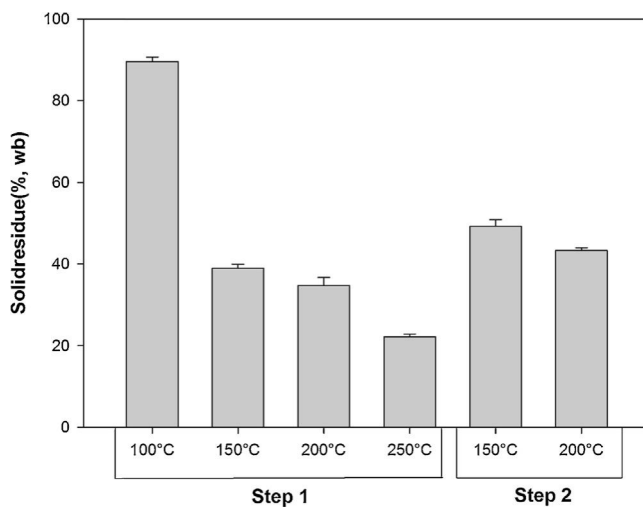


Fig. 5. Solid residue left inside the reactor after the subcritical water hydrolysis of sugarcane bagasse.

in hydrolysate pH is observed at higher temperatures, consistent with the presence of higher concentrations of organic acids in the hydrolysate at these conditions. In terms of dynamics, the pH of aqueous solution decreases sharply during the first 10 min of hydrolysis and then levels off. The minimum pH achieved here was 3.43, observed for a hydrolysis temperature of 250 °C [35,43,44]. The weakly acidic hydrolysate pH shown in Fig. 4 for temperatures of 100 and 150 °C is consistent with the observation that these

lower temperatures are insufficient for hydrolysis of the lignocellulosic complex.

3.4. Residual solid

The amount of residual solid after steps 1 and 2 of subcritical water treatment was quantified and analyzed. Visually, the residue appears to consist of un-reacted sugarcane bagasse, carbonized sugarcane bagasse, hydrolyzed but still insoluble parts of sugarcane bagasse as well as inorganic compounds. The masses of residual solids remaining after steps 1 and 2 are shown in Fig. 5. The amount of residual solids decreased with increasing temperature as expected based on the hydrolysate measurements; by contrast, the TRS yield increased with increasing temperature. The mass of residual solids produced during step 1 decreased drastically from 80% (at 100 °C) to 20% (at 250 °C), which parallels the increase in TRS yield shown in Fig. 2. The sharp decrease in solids yield is consistent with the ability of subcritical water to decompose insoluble macromolecules of sugarcane bagasse into smaller soluble compounds in a short residence time [35]. Fig. 5 also shows that the mass of residual solid remaining at the end of step 2 was approximately the same as the one found after step 1, and accounted for approximately 45% of the initial raw material. For sugarcane bagasse semi-continuous hydrolysis at approximately 200 °C and treatment times ranging from 4 to 15 min, solid yields ranging from about 40 to 60% have been reported [27,28]. There was not a considerable difference between the final amounts of remaining solids obtained at temperatures of 150 and 200 °C following step 2 (43% and 49%, respectively), which suggests that the sugarcane bagasse was not completely hydrolyzed.

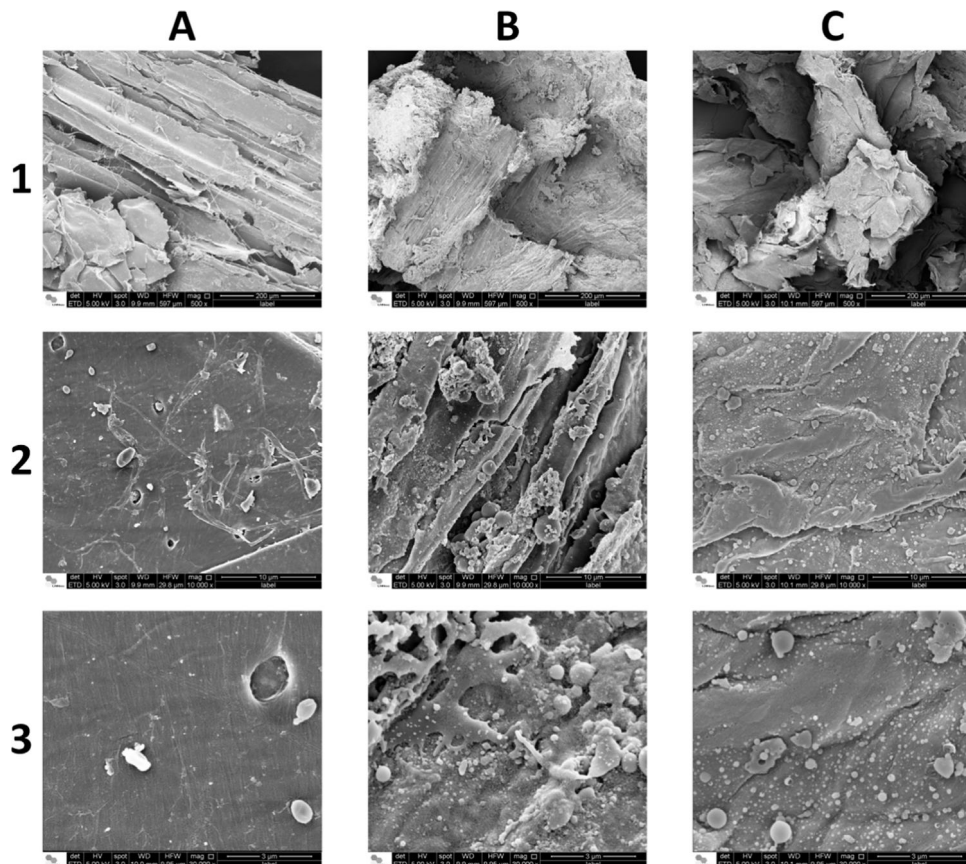


Fig. 6. Images obtained by FESEM on the surface of sugarcane bagasse analyzed before (column A) and after the subcritical water hydrolysis at 150 °C and 10 MPa (column B) and at 100 °C and 10 MPa (column C) at different magnifications. Scale bar: 200 μm (row 1); 10 μm (row 2); 3 μm (row 3).

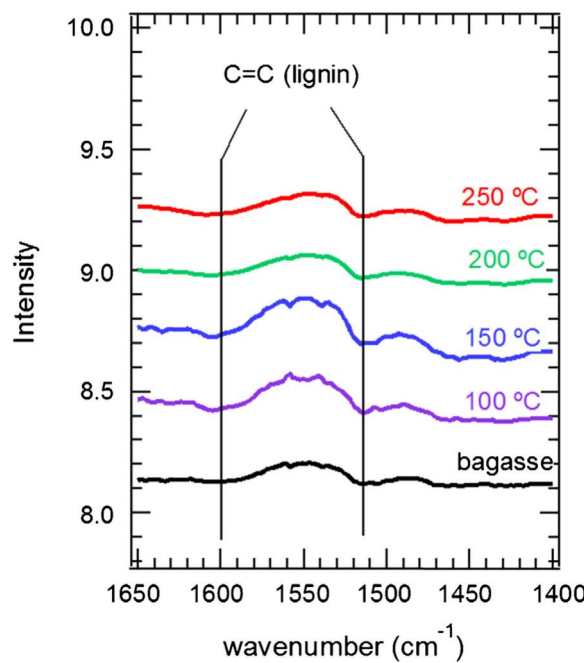


Fig. 7. DRIFT spectra analysis of sugarcane bagasse in the aromatic C=C stretching region (1650–1400 cm⁻¹).

3.4.1. Field emission scanning electron microscopy

The Fig. 6 shows images of FESEM of sugarcane bagasse samples obtained before (column A) and after SWH at 150 °C and 10 MPa (column B) and at 100 °C and 10 MPa (column C) at different magnifications. The morphology of the sugarcane bagasse residue was clearly influenced by the SWH treatment. The surface of the non-treated bagasse presents a morphology consistent with the native sugarcane cell wall, with visible parallel conducting vessels (row 1-A). After SWH, the bagasse particles appear twisted and disrupted (row 1-B and 1-C). At higher magnification (rows 2 and 3), the relatively flat surface observed in the untreated sample appear to become more degraded and covered by particulate material. Interestingly, hydrolysis at 150 °C disrupted the lignocellulosic structure more extensively than the treatment at 100 °C, despite the fact that the TRS yield did not increase between 100 and 150 °C. We interpret this observation as suggesting that treatment at 150 °C is sufficient for disrupting the physical structure of sugarcane bagasse but that the temperature is insufficient for bond hydrolysis at the treatment times studied here.

3.4.2. Diffuse reflectance infrared Fourier transform spectroscopy

The chemical composition of the residual solids was characterized for functional group content using DRIFTS. The aim of the DRIFTS characterization tests was to corroborate the TRS yield and pH data and to gain understanding of the composition of the residual bagasse. Fig. 7 shows the spectral region from 1650 to 1400 cm⁻¹ that has been associated primarily with the aromatic C=C bonds present in lignin [30,45]. Starting at a hydrolysis temperature of 100 °C, bands at 1600 and 1510 cm⁻¹ start becoming more prominent and distinct. Likewise, minor bands at 1460 and 1430 cm⁻¹, associated with aromatic C–H bends [30,45], become more prominent with increasing hydrolysis temperature. Interestingly, the lignin features become less distinct at hydrolysis temperature of 200 and 250 °C, which may be attributable to deposition of secondary products on the lignin surface.

Fig. 8 shows the spectral region from 1800 to 1600 cm⁻¹ that is well known to contain information about carbonyls [46]. Here, the carbonyl stretch, originally present as a strong band

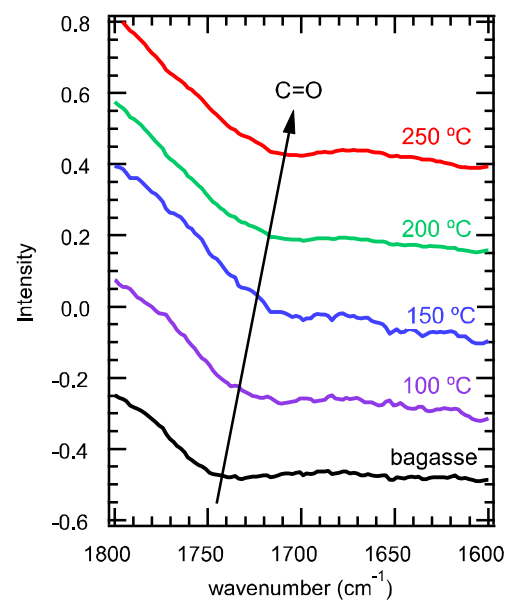


Fig. 8. DRIFT spectra analysis of sugarcane bagasse in the carbonyl C=O stretching region (1800–1600 cm⁻¹).

at approximately 1740 cm⁻¹ decreases in intensity and shifts to lower wavenumbers with increasing hydrolysis temperature. These observations are consistent with hydrolytic stripping of acetyl sidechains present on hemicellulose, preferentially leaving behind primarily ketones and aldehyde groups present in lignin [45]. This should be connected back to the observed drop in pH of the hydrolysate as the acetyl sidechains produce acetic acid, one of the main acids responsible for H⁺.

Fig. 9 shows the spectral region from 3100 to 2700 cm⁻¹, a region typically associated with C–H stretching modes [46]. Following assignments from Russo, Stanzone, Tregrossi and Ciajolo [47], we can assign the individual bands associated with CH, CH₂, and CH₃ stretches; in all cases, the C–H stretching peaks become more distinct with increasing hydrolysis

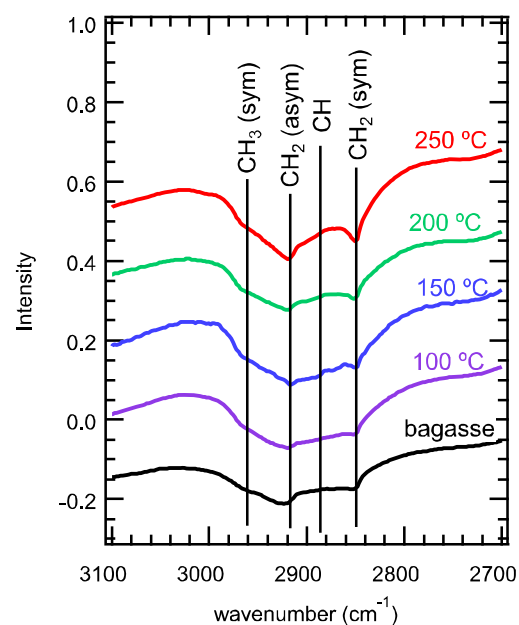


Fig. 9. DRIFT spectra analysis of sugarcane bagasse in the C–H stretching region (3100–2700 cm⁻¹).

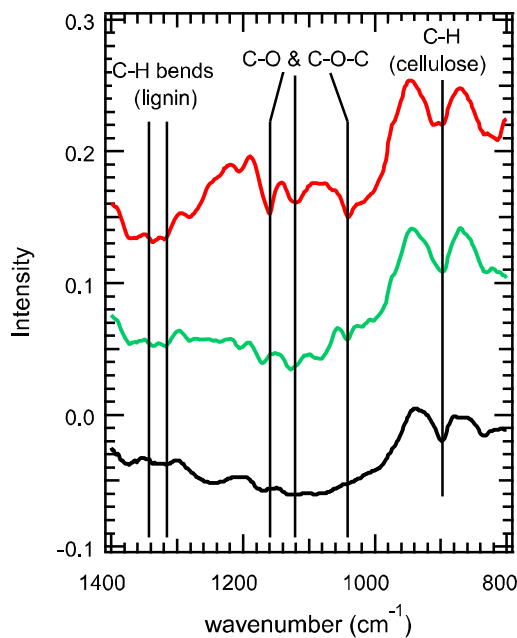


Fig. 10. DRIFT spectra analysis of sugarcane bagasse C–O and other important biomass functional groups stretching region (1400–800 cm⁻¹).

temperature, consistent with removal of hemicellulose and possibly cellulose components that leaves a less complex mixture of C–H bonds in the residual solid. The aromatic C–H stretch typically present at approximately 3040 cm⁻¹ [47] is not observed in any of the samples, and we attribute this to the presence of the broad O–H stretch which obscures the aromatic C–H stretch.

Finally, Fig. 10 shows the spectral region from 1400 to 800 cm⁻¹ that is associated with C–O stretches [46] and other important biomass functional groups [30,45,48]. Again, the individual bands associated with C–O–C linkages at 1160 cm⁻¹ [30] and 1115 cm⁻¹ [49] become more distinct with increasing temperature, consistent with hydrolytic removal of hemicellulose and possibly amorphous cellulose components. The persistence of the band at 900 cm⁻¹, associated with C–H deformation in cellulose [30], and the bands at approximately 840 cm⁻¹, associated with D-glycosidic bonds [48], suggests that hydrolysis does not remove all cellulose components; based on its known recalcitrance, we suggest that the residual cellulose is primarily crystalline.

3.5. Severity factor

The severity factor was calculated from Eq. (2) for step 1. Fig. 11 shows the variation in the yields of TRS with log(R₀). The single step 1 pretreatment was conducted at four different temperatures ranging from 100 to 250 °C, corresponding to severity factors ranging from 1.04 to 5.41. Under moderate conditions, SWH produces long-chain oligomers, which are reduced in length by increasing the severity [40,50–52]. The treatment performed at 200 °C/5 MPa showed severity of 3.9 corroborating literature similar data for severity factor in those conditions [27,53]. The treatment at 250 °C showed the highest value of severity 5.9, moreover, the high temperature collapsed the lignocellulosic structure; the recovery of cellulose generally decreases with increasing severity [54].

The severity factor described in the Eq. (2) can only be used if the temperature remains constant during the reaction; in the case of the step 2 significant heat-up times were noticed, a modified severity factor was used, which considers integrating the temperature profile during heat up.

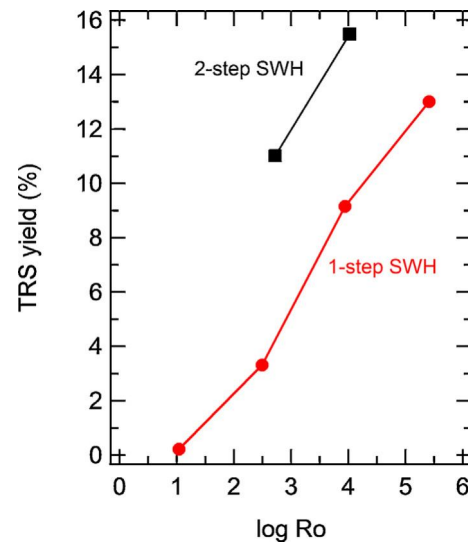


Fig. 11. Yields of TRS for step 1 and step 2 vs. log(R₀).

$$R_0 = \int_0^t \exp\left(\frac{T(t) - 100}{14.75}\right) dt \quad (5)$$

where all symbols retain their previous definitions [55].

Fig. 11 also shows the variation in the yields of TRS with log(R₀) for step 2, which makes more obvious that log(R₀) does not capture the differences between the two methods. Maybe this is as a result of the severity model used does not include the pH in the equation.

Sugar degradation increases with increasing severity factor. Therefore, balancing between hydrolysis efficiency and sugars yield is necessary. When the aim of SWH is to produce fermentable sugars, the factor severity should be decreased to avoid sugars degradation, especially considering that many degradation products are fermentation inhibitors. Here, we are aiming to use SWH to produce a liquid feed for gasification, shifting the objectives. Specifically, primary sugar degradation products (furfural-based compounds, organic acids, and similar) can be gasified under supercritical water conditions. However, accumulation of high concentrations of degradation products can lead to formation of insoluble secondary products (humins), resulting in downstream operational problems (e.g., clogging of valves, etc.). Therefore, while the motivations are different, optimization of the severity factor either as a pre-processing step for fermentation or gasification requires balancing biomass hydrolysis with sugar degradation.

4. Conclusions

SWH was studied as a semi-batch technology for valorizing sugarcane bagasse waste biomass. The specific focus of this study was to understand the SWH process as a means to produce a water-soluble carbon-rich product stream amenable for continuous production of fuel gas via supercritical gasification. The proposed SWH-gasification technology reduces problems associated with solids feeding into high-temperature/high-pressure gasifier reactors; instead, the solids can be fed under semi-batch conditions into the SWH reactor and several SWH reactors can be operated in parallel to simulate continuous feed to a single gasifier. Accordingly, the studied included examinations of dynamic temperature profiles, and biomass holding times on TRS yields, hydrolysate pH, and composition of the residual solids. In addition, we tested two reactor protocols, one consisting entirely of dynamic flow, the other consisting of a static period followed by

flow. In both cases, we found that increasing the SWH temperature from 100 to 250 °C increased the measured TRS yield. For the 1-step process, the highest TRS yield was obtained as 13% after 20 minutes at 250 °C. For the 2-step process, the highest TRS yield was 15.9%, again after 20 min of flow conditions but at 200 °C (the highest temperature examined). The increased TRS yields obtained for the 2-step process were consistent with lower amounts of sugar degradation, as measurements of the residual solid mass indicated that the 1-step process hydrolyzed a larger fraction of the biomass than did the 2-step process. In all cases, hydrolyze pH decreased to a minimum value less than 4, an important consideration for corrosion-resistant design of downstream process components. The residual biomass was characterized using electron microscopy and DRIFTS. These tests confirmed structural disruption of the biomass and indicated that SWH treatment achieved hemicellulose and (potentially) partial cellulose hydrolysis; bands associated with lignin did not disappear during SWH treatment, consistent with their known stability at the conditions examined here.

Acknowledgments

The authors acknowledge the financial support from Fundação de Amparo à Pesquisa do Estado de São Paulo – FAPESP (2011/19817-1) and the LME/LNNano/CNPEM for technical support during the electron microscopy analysis.

References

- [1] L. Faba, E. Díaz, S. Ordóñez, Recent developments on the catalytic technologies for the transformation of biomass into biofuels: a patent survey, *Renew. Sustain. Energy Rev.* 51 (2015) 273–287.
- [2] R. Lin, J. Cheng, L. Ding, W. Song, F. Qi, J. Zhou, K. Cen, Subcritical water hydrolysis of rice straw for reducing sugar production with focus on degradation by-products and kinetic analysis, *Bioresour. Technol.* 186 (2015) 8–14.
- [3] UNICA, União da Indústria de cana de açúcar, 2015.
- [4] C.R. Soccol, L.P. Vandenberghe, A.B. Medeiros, S.G. Karp, M. Buckeridge, L.P. Ramos, A.P. Pitarello, V. Ferreira-Leitao, L.M. Gottschalk, M.A. Ferrara, E.P. da Silva Bon, L.M. de Moraes, A. Araujo Jde, F.A. Torres, Bioethanol from lignocelluloses: status and perspectives in Brazil, *Bioresour. Technol.* 101 (2010) 4820–4825.
- [5] J.M. Prado, L.A. Follegatti-Romero, T. Forster-Carneiro, M.A. Rostagno, F. Maugeri Filho, M.A.A. Meireles, Hydrolysis of sugarcane bagasse in subcritical water, *J. Supercrit. Fluids* 86 (2014) 15–22.
- [6] G. Zhu, Z. Xiao, X. Zhu, F. Yi, X. Wan, Reducing sugars production from sugarcane bagasse wastes by hydrolysis in sub-critical water, *Clean Technol. Environ. Policy* 15 (2013) 55–61.
- [7] M. Saska, E. Ozer, Aqueous extraction of sugarcane bagasse hemicellulose and production of xylose syrup, *Biotechnol. Bioeng.* 45 (1995) 517–523.
- [8] L.A.R. Batalha, Q. Han, H. Jameel, H.-m. Chang, J.L. Colodette, F.J. Borges Gomes, Production of fermentable sugars from sugarcane bagasse by enzymatic hydrolysis after autohydrolysis and mechanical refining, *Bioresour. Technol.* 180 (2015) 97–105.
- [9] A.P. Ramón, L. Taschetto, F. Lunelli, E.T. Mezadri, M. Souza, E.L. Foletto, S.L. Jahn, R.C. Kuhn, M.A. Mazutti, Ultrasound-assisted acid and enzymatic hydrolysis of yam (*Dioscorea sp.*) for the production of fermentable sugars, *Biocat. Agric. Biotechnol.* 4 (2015) 98–102.
- [10] L. Jiang, A. Zheng, Z. Zhao, F. He, H. Li, W. Liu, Obtaining fermentable sugars by dilute acid hydrolysis of hemicellulose and fast pyrolysis of cellulose, *Bioresour. Technol.* 182 (2015) 364–367.
- [11] G. Brunner, Supercritical fluids: technology and application to food processing, *J. Food Eng.* 67 (2005) 21–33.
- [12] A. Kruse, E. Dinjus, Hot compressed water as reaction medium and reactant: properties and synthesis reactions, *J. Supercrit. Fluids* 39 (2007) 362–380.
- [13] J.B. Gadhe, R.B. Gupta, Hydrogen production by methanol reforming in supercritical water: suppression of methane formation, *Ind. Eng. Chem. Res.* 44 (2005) 4577–4585.
- [14] A.J. Byrd, K. Pant, R.B. Gupta, Hydrogen production from ethanol by reforming in supercritical water using Ru/Al₂O₃ catalyst, *Energy Fuels* 21 (2007) 3541–3547.
- [15] D. Yu, M. Aihara, M.J. Antal Jr., Hydrogen production by steam reforming glucose in supercritical water, *Energy Fuels* 7 (1993) 574–577.
- [16] F. Fisher, H. Tropsch, P. Dilthey, *Brennst. Chem.* 6 (1925) 265.
- [17] H. Yoshida, K. Watanabe, N. Iwasa, S.-i. Fujita, M. Arai, Selective methanation of CO in H₂-rich gas stream by synthetic nickel-containing smectite based catalysts, *Appl. Catal. B: Environ.* 162 (2015) 93–97.
- [18] S.I. Sandler, Chemical, Biochemical, in: and Engineering Thermodynamics, 4th ed., John Wiley & Sons, NJ, 2006.
- [19] R.P. Overend, E. Chornet, J.A. Gascoigne, Fractionation of lignocellulosics by steam-aqueous pretreatments [and discussion], *Philos. Trans. R. Soc. Lond. A: Math. Phys. Eng. Sci.* 321 (1987) 523–536.
- [20] E. Chornet, R.P. Overend, Phenomenological kinetics and reaction engineering aspects of steam/aqueous treatments, in: B. Focher, A. Marzetti, V. Crescenzi (Eds.), *Steam Explosion Techniques: Fundamentals and Industrial Applications*, Goran and Breach Science Publishers, New York, 1991, pp. 21–58.
- [21] N. Nelson, A photometric adaptation of the Somogyi method for the determination of glucose, *J. Biol. Chem.* 153 (1944) 375–380.
- [22] G.L. Miller, Use of dinitrosalicylic acid reagent for determination of reducing sugar, *Anal. Chem.* 31 (1959) 426–428.
- [23] D. Ciftci, M.D.A. Saldaña, Hydrolysis of sweet blue lupin hull using subcritical water technology, *Bioresour. Technol.* 194 (2015) 75–82.
- [24] D.A. Cantero, A. Sánchez Tapia, M.D. Bermejo, M.J. Cocco, Pressure and temperature effect on cellulose hydrolysis in pressurized water, *Chem. Eng. J.* 276 (2015) 145–154.
- [25] F.P. Cardenas-Toro, T. Forster-Carneiro, M.A. Rostagno, A.J. Petenate, F. Maugeri Filho, M.A.A. Meireles, Integrated supercritical fluid extraction and subcritical water hydrolysis for the recovery of bioactive compounds from pressed palm fiber, *J. Supercrit. Fluids* 93 (2014) 42–48.
- [26] G. Garrote, H. Dominguez, J. Parajo, Hydrothermal processing of lignocellulosic materials, *Eur. J. Wood Wood Prod.* 57 (1999) 191–202.
- [27] W.S.L. Mok, M.J. Antal Jr., Uncatalyzed solvolysis of whole biomass hemicellulose by hot compressed liquid water, *Ind. Eng. Chem. Res.* 31 (1992) 1157–1161.
- [28] S.G. Allen, I.C. Kam, A.J. Zemann, M.J. Antal, Fractionation of sugar cane with hot, compressed, liquid water, *Ind. Eng. Chem. Res.* 35 (1996) 2709–2715.
- [29] T. Sakaki, M. Shibata, T. Sumi, S. Yasuda, Saccharification of cellulose using a hot-compressed water-flow reactor, *Ind. Eng. Chem. Res.* 41 (2002) 661–665.
- [30] X. Lü, S. Saka, Hydrolysis of Japanese beech by batch and semi-flow water under subcritical temperatures and pressures, *Biomass Bioenergy* 34 (2010) 1089–1097.
- [31] G. Brunner, Near critical and supercritical water. Part I. Hydrolytic and hydrothermal processes, *J. Supercrit. Fluids* 47 (2009) 373–381.
- [32] C. Schacht, C. Zetzl, G. Brunner, From plant materials to ethanol by means of supercritical fluid technology, *J. Supercrit. Fluids* 46 (2008) 299–321.
- [33] H. Ando, T. Sakaki, T. Kokusho, M. Shibata, Y. Uemura, Y. Hatate, Decomposition behavior of plant biomass in hot-compressed water, *Ind. Eng. Chem. Res.* 39 (2000) 3688–3693.
- [34] S.S. Toor, L. Rosendahl, A. Rudolf, Hydrothermal liquefaction of biomass: a review of subcritical water technologies, *Energy* 36 (2011) 2328–2342.
- [35] O. Pourali, F.S. Asghari, H. Yoshida, Production of phenolic compounds from rice bran biomass under subcritical water conditions, *Chem. Eng. J.* 160 (2010) 259–266.
- [36] W. Abdelmoez, S.M. Nage, A. Bastawess, A. Ihab, H. Yoshida, Subcritical water technology for wheat straw hydrolysis to produce value added products, *J. Clean. Prod.* 70 (2014) 68–77.
- [37] G. Zhu, X. Zhu, Q. Fan, X. Wan, Production of reducing sugars from bean dregs waste by hydrolysis in subcritical water, *J. Anal. Appl. Pyrolysis* 90 (2011) 182–186.
- [38] J.M. Prado, T. Forster-Carneiro, M.A. Rostagno, L.A. Follegatti-Romero, F. Maugeri Filho, M.A.A. Meireles, Obtaining sugars from coconut husk, defatted grape seed, and pressed palm fiber by hydrolysis with subcritical water, *J. Supercrit. Fluids* 89 (2014) 89–98.
- [39] C. Liu, C.E. Wyman, Impact of fluid velocity on hot water only pretreatment of corn stover in a flowthrough reactor, in: *Proceedings of the Twenty-Fifth Symposium on Biotechnology for Fuels and Chemicals, May 4–7, 2003, in Breckenridge, CO*, Springer, 2004, pp. 977–987.
- [40] C. Liu, C.E. Wyman, The effect of flow rate of compressed hot water on xylan, lignin, and total mass removal from corn stover, *Ind. Eng. Chem. Res.* 42 (2003) 5409–5416.
- [41] M. Tanaka, A. Takamizu, M. Hoshino, M. Sasaki, M. Goto, Extraction of dietary fiber from Citrus junos peel with subcritical water, *Food Bioprod. Process.* 90 (2012) 180–186.
- [42] W. Vermerris, R.L. Nicholson, *Phenolic Compound Biochemistry*, Springer Science & Business Media, 2007.
- [43] O. Pourali, F.S. Asghari, H. Yoshida, Sub-critical water treatment of rice bran to produce valuable materials, *Food Chem.* 115 (2009) 1–7.
- [44] F. Salak Asghari, H. Yoshida, Acid-catalyzed production of 5-hydroxymethyl furfural from D-fructose in subcritical water, *Ind. Eng. Chem. Res.* 45 (2006) 2163–2173.
- [45] A. Guilherme, P. Dantas, E. Santos, F. Fernandes, G. Macedo, Evaluation of composition, characterization and enzymatic hydrolysis of pretreated sugar cane bagasse, *Braz. J. Chem. Eng.* 32 (2015) 23–33.
- [46] R.M. Silverstein, G.C. Bassley, T.C. Morrill, *Spectrometric Identification of Organic Compounds*, 5th ed., Wiley, New York, 1991.
- [47] C. Russo, F. Stanzione, A. Tregrossi, A. Ciajolo, Infrared spectroscopy of some carbon-based materials relevant in combustion: qualitative and quantitative analysis of hydrogen, *Carbon* 74 (2014) 127–138.

- [48] F. Xu, J.X. Sun, C.F. Liu, R.C. Sun, Comparative study of alkali- and acidic organic solvent-soluble hemicellulosic polysaccharides from sugarcane bagasse, *Carbohydr. Res.* 341 (2006) 253–261.
- [49] A.B. Fuertes, M.C. Arbestain, M. Sevilla, J.A. Maciá-Agulló, S. Fiol, R. López, R.J. Smernik, W.P. Aitkenhead, F. Arce, F. Macias, Chemical and structural properties of carbonaceous products obtained by pyrolysis and hydrothermal carbonisation of corn stover, *Soil Res.* 48 (2010) 618–626.
- [50] M. Sasaki, Z. Fang, Y. Fukushima, T. Adschari, K. Arai, Dissolution and hydrolysis of cellulose in subcritical and supercritical water, *Ind. Eng. Chem. Res.* 39 (2000) 2883–2890.
- [51] M. Nagamori, T. Funazukuri, Glucose production by hydrolysis of starch under hydrothermal conditions, *J. Chem. Technol. Biotechnol.* 79 (2004) 229–233.
- [52] G.P. van Walsum, H. Shi, Carbonic acid enhancement of hydrolysis in aqueous pretreatment of corn stover, *Bioresour. Technol.* 93 (2004) 217–226.
- [53] M. Rubio, J.F. Tortosa, J. Quesada, D. Gómez, Fractionation of lignocellulosics. Solubilization of corn stalk hemicelluloses by autohydrolysis in aqueous medium, *Biomass Bioenergy* 15 (1998) 483–491.
- [54] M.Ø. Petersen, J. Larsen, M.H. Thomsen, Optimization of hydrothermal pretreatment of wheat straw for production of bioethanol at low water consumption without addition of chemicals, *Biomass Bioenergy* 33 (2009) 834–840.
- [55] T. Rogalinski, T. Ingram, G. Brunner, Hydrolysis of lignocellulosic biomass in water under elevated temperatures and pressures, *J. Supercrit. Fluids* 47 (2008) 54–63.